All-adaptive blind matched filtering for the equalization and identification of multipath channels: a practical approach

Coskun A and Kale I

This is a copy of the author's accepted version of a paper subsequently published in *IEEE Transactions on Circuits and Systems I: Fundamental Theory and Applications* 60 (1) 232-242 1057-7122.

It is available online at:

https://dx.doi.org/10.1109/TCSI.2012.2215711

All-Adaptive Blind Matched Filtering for the Equalization and Identification of Multipath Channels - A Practical Approach

Adem Coskun and Izzet Kale, *Member, IEEE*,

***Abstract*—Blind matched filter receiver is advantageous over the state-of-the-art blind schemes due the simplicity in its implementation. To estimate the multipath communication channels, it uses neither any matrix decomposition methods nor statistics of the received data higher than the second order ones. On the other hand, the realization of the conventional blind matched filter receiver requires the noise variance to be estimated and the equalizer parameters to be calculated in state-space with relatively costly matrix operations. In this paper, a novel architecture is proposed to simplify a potential hardware implementation of the blind matched filter receiver. Our novel approach transforms the blind matched filter receiver into an all-adaptive format which replaces all the matrix operations. Furthermore, the novel design does not need for any extra step to estimate the noise variance. In this paper we also report on a comparative channel equalization and channel identification scenario, looking into the performances of the conventional and our novel all-adaptive blind matched filter receiver through simulations.**

***Index Terms*—Blind Channel Estimation, Blind Channel Equalization, Constant Modulus Algorithm (CMA), Single Input Single Output (SISO) Channels .**

I. INTRODUCTION

Multipath fading is one of the major problems in wireless communication channels. Due to scattering, reflection and diffraction occurring within the channel, the transmitted signal arrives at the receiver through a number of multiple paths. If the coherence bandwidth of the channel gets lower than the signal bandwidth, due to multipath fading, the symbols transmitted at each symbol period spread over other signals in the adjacent symbol periods. This type of interference is called Inter-Symbol Interference (ISI). The estimation of the Channel Impulse Response (CIR), which carries the information on the multipath components, and the equalization of the communication channel play an important role in furnishing an ISI free signal transmission.

The Blind Matched Filter (BMF) receiver [1], [2] aims to implement Forney's receiver [3], which is the optimum receiver in the presence of ISI and Additive White Gaussian Noise (AWGN), blindly without the need for the explicit knowledge of the CIR. For this purpose the BMF approach makes use of an adaptive filter, updated via a computationally simple algorithm i.e. the Constant Modulus Algorithm (CMA). With the incorporation of the CMA into the blind CIR estimation process;

1) The communication doesn't depend on the transmission of training signals, as the use of training symbols, which are carrying no valuable information, making them inherently inefficient and wasting the bandwidth of the communication channel as well as resources at both ends, and
2) Neither matrix decomposition methods, which are implementation inefficient and expensive (such as [4],[5] using Singular Value Decomposition (SVD) and [6], [7],[8] using Eigen Value Decomposition (EVD)) nor higher order cumulant functions of the received data, e.g. [9], [10], which eventually leads to the need for long data records for accurate estimation of higher-order statistics of the received signal, were needed.

BMF is also applicable to space-time communications [11] and its convergence speed and accuracy has further been enhanced in [12]. Good references on the conventional ways for the identification of the communication channels blindly are [13] and [14].

Over the past few years, many novel blind channel estimation methods were proposed for various communication scenarios. In the recent studies matrix decomposition methods are still a need, such as [15] and [16] for Multiple Input Multiple Output Orthogonal Frequency Division Multiplexing (MIMO-OFDM), [17] for Multi-Carrier Code Division Multiple Access (MC-CDMA) systems and [18] for MIMO single-carrier zero-padding block-transmission systems. On the other hand, recursive methods for blind channel estimation needs for multiple antennas or over-sampling at the receiver end [19]. Therefore, for Single Input Single Output (SISO) channels, the BMF receiver is still advantageous in terms of computational complexity over the state-of-the-art blind channel estimation methods due to the use of the CMA in its blind matched filter estimation process.

Apart from the adaptive filtering block that implements the CMA, the BMF receiver is also composed of a linear channel equalizer block, the parameters of which have to be calculated by making use of the auto-correlation of the CIR. Although the structural simplicity appears to be the most striking feature of the BMF receiver due to the use of the CMA, the calculation of the filter parameters of the channel equalizer is performed deploying state-space operations, including matrix inversion.

The authors are with the Applied DSP and VLSI Research Group (ADVRG), School of Electronics and Computer Science, University of Westminster, W1W 6UW, London, U.K. (e-mail: adem@alptron.com; kalei@wmin.ac.uk).

In this paper we propose an all-adaptive BMF receiver discarding the need for any matrix operation, where the equalizer parameters are found via a recursive algorithm. Operations such as matrix inversion have complexity of order J^3 for a $J\times J$ matrix (See Table I in [20]). On the other hand, the recursive algorithms like Least Mean Square (LMS) and CMA have a complexity order of J when the size of the recursive filter is set to J. The estimation of the noise variance is also no longer required in our novel receiver where it is an essential component in the conventional design of the BMF receiver. In general the all adaptive design is applicable to Single Input Single Output (SISO) communication channels, where there is no need for over-sampling or introducing space diversity.

In the next section the channel model, adopted throughout the paper, will be explained. Section III presents a detailed derivation and explanation on how our novel all-adaptive BMF receiver works. An extensive set of simulations will be given in Section IV, demonstrating the validity and viability of our novel approach, with the final section being dedicated to conclusions.

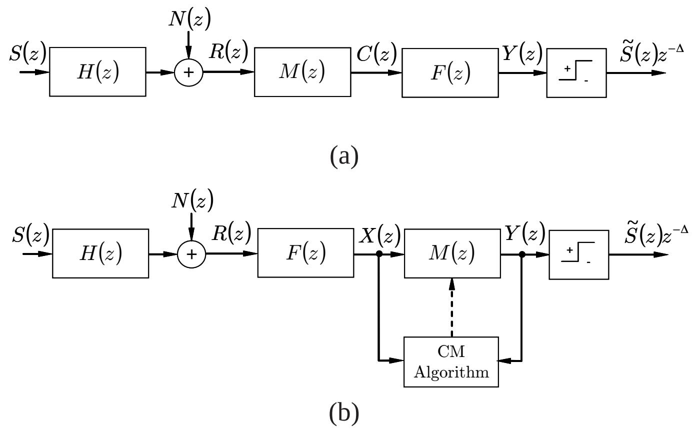

Fig. 1. (a) System model for the matched filter receiver (b) System model for the BMF receiver, where the channel equalizer $F(z)$ is placed prior to the channel matched filter $M(z)$. The filtered signal from the matched filter is applied to a decision device in order to obtain the estimate of the transmitted data stream . Δ is the equalization delay.

II. Channel Model

We assume a Single Input Single Output (SISO) communications scenario, where a single transmit and a single receive antenna are present at the transmission ends. The communication channel is assumed to be frequency selective where the number of the multipath components, L, is already known to the receiver. The received data vector, $\mathbf{r}(k)$, can be formulated as follows,

$$\mathbf{r}(k) = \mathbf{H}\times\mathbf{s}(k)+\mathbf{n}(k), \tag{1}$$

where $\mathbf{r}(k)$ represents the vector of received symbols of size $W\times 1$, i.e. $\mathbf{r}(k) = [r(k),\ r(k-1),\cdots,\ r(k-W+1)]^T$. Note that lower case **bold** characters represent the vectors and upper case bold characters represent the matrices, while $italic$ characters represent scalars in the time domain. The superscript $(\cdot)^T$ is the vector transpose and k is the discrete time index for $0\leq k\leq D-1$. D is the duration for the whole channel activity and it is the same for the duration of the whole signal transmission and signal reception. Brackets $[\cdot]$ contain the elements of a vector or a matrix and W is the length of the filter that $\mathbf{r}(k)$ is processed with. In this paper this filter is either the channel matched filter or the channel equalizer.

Similar to $\mathbf{r}(k)$, the noise vector $\mathbf{n}(k)$ is also of size $W\times 1$ which is assumed to have zero mean white Gaussian characteristics with $E\{\mathbf{n}(k)\mathbf{n}^H(k)\} = \sigma_n^2\mathbf{I}_{W,W}$, where σ_n^2 is the noise variance and $\mathbf{I}_{W,W}$ is the identity matrix of size $W\times W$. The vector of transmit symbols is $\mathbf{s}(k) = [s(k),\ s(k-1),\cdots,\ s(k-L-W+1)]^T$, of size $(L+W)\times 1$ which are independent and identically-distributed (i.i.d.), i.e. $E\{\mathbf{s}(k)\mathbf{s}^H(k)\} = \sigma_s^2\mathbf{I}_{L+W,L+W}$. $E\{\cdot\}$ is the mathematical expectation and $(\cdot)^H$ is the Hermitian transpose. The time-invariant transmission channel matrix $\mathbf{H}$ of size $W\times(L+W)$ can be represented as

$$\mathbf{H} = \begin{bmatrix} h(0) & \cdots & h(L) & 0 & \cdots & 0 \\ 0 & h(0) & \cdots & h(L) & & \vdots \\ \vdots & & \ddots & \ddots & \ddots & 0 \\ 0 & \cdots & 0 & h(0) & \cdots & h(L) \end{bmatrix} \tag{2}$$

and $\mathbf{h} = [\ h(0),\quad h(1),\quad \cdots,\quad h(L)\ ]\triangleq h(0)+h(1)z^{-1}+ ...+h(L)z^{-L} = H(z)$. Therefore, the communication scenario given in (1) can also be formulated in the z-domain as

$$\begin{aligned} R(z) &= \sum_{k=0}^{D-1} r(k)z^{k-D+1} \\ &= H(z)S(z)+N(z). \end{aligned} \tag{3}$$

$\mathbf{H}$ is in the form of a convolution matrix and for the sake of simplicity a convolution matrix will simply be represented with the notation $\mathcal{C}onv$, e.g. $\mathbf{H} = \mathcal{C}onv(H(z))$, in this paper. The representations in z-domain will be in italic capitals as in (3).

III. All-Adaptive Blind Matched Filter Receiver

The matched filter receiver is shown in Fig.1(a). The receiver is formed of two processing blocks; the channel matched filter $M(z)$ and the channel equalizer $F(z)$. Because both $M(z)$ and $F(z)$ represent linear filters, their positions can be exchanged as in Fig.1(b), to form the BMF receiver. Once the receiver is as in Fig.1(b), $M(z)$ can be estimated via the CMA. The advantages of using this type of receiver is that

- The matched filter, consequently the channel response, is extracted accommodating the CMA, which is known to be one of the simplest blind schemes
- The channel is equalized without a need for an extra hardware for channel equalization.

On the other hand, for the realization of $F(z)$, the BMF receiver necessitates the use of matrix operations (see equation (8) in [1] as repeated in Appendix A, which will be re-visited further in this paper). In this section, we report on our novel all-adaptive BMF receiver, where both $M(z)$ and $F(z)$ are estimated adaptively. In Section III.A we shall look at the derivation of the FIR all-adaptive BMF receiver and in III.B the findings will be extended to establish an IIR model for the all-adaptive BMF. Section III.C summarizes the novel all-adaptive approach with some remarks and discussions on its use.

A. FIR All-adaptive BMF Receiver

Filtering $R(z)$ with $F(z)$, as shown in Fig.1(b), gives

$$\begin{aligned} X(z) &= F(z)R(z) \\ &= F(z)H(z)S(z) + F(z)N(z). \end{aligned} \quad (4)$$

If $M(z)$ is to be designed as a Minimum Mean Squared Error (MMSE) equalizer, then $M(z)$ should satisfy the orthogonality principle $E\{(M(z)X(z) - S(z))\bar{X}(z)\} = 0$, which leads to

$$\begin{aligned} M(z) &= E\{S(z)\bar{X}(z)\}E\{X(z)\bar{X}(z)\}^{-1} \\ &= \Phi_{SX}(\Phi_{XX})^{-1}. \end{aligned} \quad (5)$$

where Φ_{XX} is the auto-correlation function for $X(z)$, which can be calculated as $\Phi_{XX} = F(z)\Phi_{RR}\bar{F}(z)$. Similarly Φ_{SX} is the cross-correlation function for $S(z)$ and $\bar{X}(z)$, where $\Phi_{SX} = \bar{F}(z)\bar{H}(z)\Phi_{SS}$. Notation $\bar{(\cdot)}$ implies paraconjugate of a transfer function, e.g. $\bar{F}(z) = F^*(\frac{1}{z^*})$. $(\cdot)^*$ denotes the conjugate operation. The autocorrelation function Φ_{SS} is defined as $\Phi_{SS} = E\{S(z)\bar{S}(z)\} = \sum_{i=-\infty}^{\infty} lim_{D\to\infty}\frac{1}{D}\{\sum_{k=0}^{D-1} s(k)s^*(k-i)\}z^{-i}$. Because $s(k)$s are i.i.d., $\Phi_{SS} = \sigma_s^2$, and similarly $\Phi_{NN} = \sigma_n^2$.

if we choose $F(z)$ to be

$$F(z) = \frac{\sigma_s^2}{\Phi_{RR}} = \frac{1}{H(z)\bar{H}(z) + \gamma} = \frac{1}{Q(z)}, \quad (6)$$

the MMSE equalizer $M(z)$ can be found as

$$M(z) = \frac{\bar{H}(z)\Phi_{SS}}{F(z)\Phi_{RR}} = \bar{H}(z), \quad (7)$$

where $\gamma = \sigma_n^2/\sigma_s^2$ and $\bar{H}(z) = \sum_{i=-L}^{0} h^*(-i)z^{-i}$.

(7) shows that, if $F(z)$ is as in (6), $M(z)$, designed in the MMSE sense, is an FIR filter and is equal to the time-reversed conjugate of $H(z)$, which is also known as the channel matched filter. The vector of coefficients for $M(z)$ are $\mathbf{m} = [m(-L), ..., m(0)]$, where $m(-i) = h^*(i)$ for $i = 0, .., L$.

On the other hand, $Q(z)$, from (6), can be estimated by setting a finite D in the autocorrelation function Φ_{RR} as

$$\tilde{Q}(z) = \frac{\tilde{\Phi}_{RR}}{\sigma_s^2} = \sum_{i=-L}^{L} \frac{\sum_{k=0}^{D-1}\{r(k)r^*(k-i)\}z^{-i}}{D\sigma_s^2}, \quad (8)$$

where $\tilde{Q}(z) = \tilde{q}(L)z^{-L} + ... + \tilde{q}(0) + ... + \tilde{q}(-L)z^L$. Terms with $\sim$ above them (as $\tilde{(\cdot)}$) represents the estimates of their corresponding vector or scalar. We can conclude from (8) that for the estimation of $Q(z)$, a simple averaging operation would be enough over the received signal as σ_s^2 is already known to the receiver.

Calculation of the FIR Equalizer Coefficients: Here we define a noise-free communication scenario similar to (3) as follows

$$R_I(z) = Q(z)S_I(z), \quad (9)$$

where $S_I(z)$ is filtered by $Q(z)$ as $R_I(z)$ is the result of the filtering operation in z-domain. Similar to (1), (9) may also be formulated as $\mathbf{r}_I(k) = \mathbf{Q} \times \mathbf{s}_I(k)$, where $\mathbf{Q} = \mathcal{C}onv(Q(z))$ and $\mathbf{r}_I(k)$ is in the same form as $\mathbf{r}(k)$ of (1). $S_I(z)$ is a white random sequence, having the same properties that $S(z)$ has. Here in this study $S_I(z)$ will be generated inside the receiver for the purpose of estimating the an FIR approximant for $F(z)$, which will be detailed later on in this section.

It is pretty obvious that $F(z) = 1/Q(z)$, as defined in (6), is also equal to the the optimum Auto-Regressive (AR) equalizer filter for the noise-free communication scenario given in (9), which simply removes the effect of $Q(z)$.

Note that the direct realization of $F(z)$ is not always possible as $F(z)$ may have poles outside the unit circle, and therefore it would be unstable. Therefore, rather than an unstable AR equalizer, here we aim to obtain the FIR approximant of $F(z)$ by setting its length to J.

A recursive algorithm in the form of the Least Mean Square (LMS) method can be introduced to estimate the tap values of the FIR approximant of the channel equalizer in the form of $F(z) = f(0) + f(1)z^{-1} + ... + f(J-1)z^{-J+1}$. If LMS step-size, χ, satisfies $0 < \chi < 2/\alpha_{max}$ and $\chi < 2/\sum_i \alpha_i$, where $\sum_i \alpha_i$ and α_{max} represents the sum of eigenvalues and the maximum eigenvalue for $\mathbf{R}_{\mathbf{r}_I\mathbf{r}_I} = E\{\mathbf{r}_I(k)\mathbf{r}_I^H(k)\}$ respectively, the LMS settles around the optimum channel equalizer $[22, page\ 26]$. Therefore $\mathbf{f} = [f(0), ..., f(J-1)]$, is estimated through the following equation;

$$\tilde{\mathbf{f}}(k+1) = \tilde{\mathbf{f}}(k) + \chi e(k)\mathbf{r}_I^H(k), \quad (10)$$

where $e(k)$ is the error calculated as $e(k) = \tilde{\mathbf{f}}(k)\times\mathbf{r}_I(k) - s_I(k-\Delta)$.

As $\mathbf{f}$ will recursively be estimated, $\tilde{\mathbf{f}}(k)$ represents the value of $\tilde{\mathbf{f}}$ at the kth iteration that takes place at the kth time instant and $\tilde{\mathbf{f}}(k+1)$ is that of value at the next iteration, i.e. at the $(k+1)$th time instant.

Constant Modulus Algorithm for Channel Matched Filter Estimation: The close relationship between the Constant Modulus (CM) and MMSE (or Wiener) equalizers is well studied in many works including [21], [22] and [23]. Therefore, we replace $M(z)$, designed as a MMSE equalizer in (5), with an adaptive filter, the coefficients of which are updated via the CMA.

The CM cost function $J_{\rm CMA}$ to be minimized is;

$$J_{\rm CMA} = \frac{1}{4}E\{(|y(k)|^2 - R_2)^2\} \text{ and } R_2 = \frac{E\{|s(k)|^4\}}{E\{|s(k)|^2\}}, \quad (11)$$

where R_2 is called the dispersion constant. Using stochastic gradient descent on $J_{\rm CMA}$, the matched filter can be updated by deploying the following formula [21];

$$\tilde{\mathbf{m}}(k+1) = \tilde{\mathbf{m}}(k) + \mu \mathbf{x}(k)^H y(k)(|y(k)|^2 - R_2). \quad (12)$$

$\mathbf{x}(k) = [x(k),\ x(k-1),\ ...,\ x(k-L)]^T$ is the vector of signal coefficients at the input of $M(z)$, where

$$x(k) = \tilde{\mathbf{f}}(k) \times \mathbf{r}(k) \quad (13)$$

and similarly $y(k) = \tilde{\mathbf{m}}(k) \times \mathbf{x}(k)$ is the output of the matched filter for the receiver depicted in Fig.1(b). μ is a small step-size.

The Error Bound Obtained Replacing the MMSE Equalizer with the CM Equalizer: Because $J_{\rm CMA}$ is not the same as the MMSE criterion, $\tilde{\mathbf{m}}$ will converge towards the MMSE solution with an error, which will be described in this part.

Based on Fig.1(b), $Y(z)$ can be formulated as, $Y(z) = M(z)X(z) = \Lambda(z)S(z) + \Omega(z)N(z)$, where $\Lambda(z) = M(z)F(z)H(z)$ and $\Omega(z) = M(z)F(z)$. $\Lambda(z)$ and $\Omega(z)$ are assumed to be Bounded Input Bounded Output (BIBO) stable IIR/FIR filters. If we represent $\Lambda(z)$ and $\Omega(z)$ with their infinite impulse responses, i.e. $\Lambda(z) = \sum_{i=-\infty}^{\infty} \lambda(i) z^{-i}$ and $\Omega(z) = \sum_{i=-\infty}^{\infty} \omega(i) z^{-i}$, the inverse of the Signal-to-Interference plus Noise Ratio (SINR) can be formulated as

$$\kappa = \frac{\sum_i |\omega(i)|^2 + \sum_{i \neq \Delta} |\lambda(i)|^2}{|\lambda(\Delta)|^2}, \quad (14)$$

where Δ is the equalization delay.

The difference between κ, when $M(z)$ is an MMSE equalizer found by (7), i.e. $\kappa_{\rm MMSE}$, and κ when the CMA in (12) is used, i.e. $\kappa_{\rm CMA}$, is [24]

$$\kappa_{\rm MMSE} - \kappa_{\rm CMA} \le \xi \kappa_{\rm MMSE}^2 + \mathcal{O}(\kappa_{\rm MMSE}^3) \quad (15)$$

where it shows that the error performance of the CMA is correlated with the performance of the MMSE equalizer with a tolerable bound and ξ is a constant being $\xi = \sigma_s^2/2$ for Binary Phase Shift Keying (BPSK) constellations.

The Adaptive Estimation of the Equalizer coefficients: The communication model in (9) can implicitly and in a simple manner be implemented within the receiver. If a random training sequence generator runs within the receiver to create $\mathbf{s}_I(k)$, a two layer filter as shown in Fig.2 can create the input signal $\mathbf{x}(k)$ to the adaptive filter formulated in (12). The block named "LMS" in Fig.2 corresponds to equation (10). The top layer in Fig.2, where $\mathbf{s}_I(k)$ is implicitly generated and $\tilde{\mathbf{f}}$ is estimated, is called the Adaptive FIR Approximant of the Auto-Regressive (AFA-AR) filter. In Fig.2 $\tilde{\mathbf{q}} = [\tilde{q}(-L), \tilde{q}(-L+1), ..., \tilde{q}(L)]$ is the vector of auto-correlation estimate of the channel output found using (8). This also shows that a separate estimate for the noise power σ_n^2 is no longer needed, contrary to the need for noise variance estimation in [1] and [12].

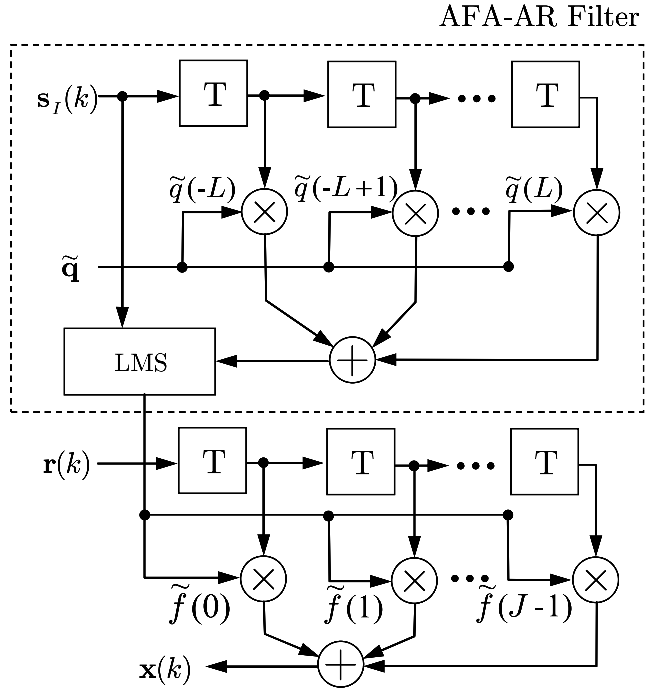

Fig. 2. The two-layer FIR filter that enables the adaptive update of $\tilde{\mathbf{f}} = [\tilde{f}(0), ..., \tilde{f}(J-1)]$. The block that estimates $\tilde{\mathbf{f}}$ is called the AFA-AR filter.

B. IIR All-adaptive BMF Receiver

In the conventional BMF design, $F(z)$ is an IIR filter, in the form of

$$F(z) = F_F(z) \times \frac{1}{F_B(z)}, \quad (16)$$

where $F_F(z) = \sum_{i=0}^{J-1} f_F(i) z^{-i}$ and $F_B(z) = 1 + \sum_{i=1}^{L} f_B(i) z^{-i}$ are the FIR transfer functions of the feedforward and the feedback filters respectively. For the conventional BMF receiver the vector of filter coefficients $\mathbf{f}_F = [f_F(0),\ ...,\ f_F(J-1)]$ and $\mathbf{f}_B = [f_B(1),\ ...,\ f_B(L)]$ are found as formulated in (36) and (38) respectively from Appendix A.

If the received signal is filtered by $M(z)$, as shown in Fig.1(a), then

$$\mathbf{c}(k) = \mathbf{M}\mathbf{r}(k) = \mathbf{M}\mathbf{H}\mathbf{s}(k) + \mathbf{M}\mathbf{n}(k), \quad (17)$$

where $\mathbf{M} = \mathcal{C}onv(M(z))$. Defining two concatenated vectors $\mathbf{f}_C = [\mathbf{f}_F, -\mathbf{f}_B]$ and $\mathbf{c}_C(k) = [\mathbf{c}^T(k), \mathbf{s}^T(k-\Delta-1)]^T$, the solution to the minimization of the MMSE cost function $E\{|\mathbf{f}_C \times \mathbf{c}_C(k) - s(k-\Delta)|^2\}$, leads to

$$\mathbf{f}_F \quad = \quad E\{s(k-\Delta)\mathbf{c}^H(k)\}(\mathbf{R_{cc}} - \frac{1}{\sigma_s^2}\mathbf{R_{sc}}^H\mathbf{R_{sc}})^{-1} \quad (18)$$

and

$$\mathbf{f}_B = \mathbf{f}_F \mathbf{R}_{\mathbf{sc}}^H \tag{19}$$

assuming that the use of $\mathbf{f}_C$ provides perfect recovery of the transmitted symbols. Note that (18) and (19) are also equal to the feedforward and feedback filters of a Decision Feedback Equalizer (DFE) [31]. $\mathbf{R}_{\mathbf{cc}}$ is the auto-correlation matrix for $\mathbf{c}(k)$ and $\mathbf{R}_{\mathbf{sc}}$ is the matrix of cross-correlation between $\mathbf{s}(k-\Delta-1)$ and $\mathbf{c}(k)$ of size $L\times 1$ and $J\times 1$ respectively.

It can be shown that (18) is equal to (36) (as provided in Appendix A) if the equalization delay Δ is set to

$$\Delta = J + L - 1. \tag{20}$$

Therefore, the conventional BMF receiver can also be derived using (18) and (19) by setting the correct Δ.

Based on (17),

$$\begin{aligned} \mathbf{R}_{\mathbf{cc}} &= E\{\mathbf{M}\mathbf{r}(k)\mathbf{r}^H(k)\mathbf{M}^H\} \\ &= \sigma_s^2 \mathbf{M}\mathbf{H}\mathbf{H}^H\mathbf{M}^H + \sigma_n^2 \mathbf{M}\mathbf{M}^H \end{aligned} \tag{21}$$

and by calling $\mathbf{P} = \mathbf{M}\mathbf{H}$

$$\mathbf{R}_{\mathbf{cc}} = \sigma_s^2 \mathbf{P}\mathbf{P}^H + \sigma_n^2 \mathbf{P}\mathbf{A}^H, \tag{22}$$

where $\mathbf{A} = [\mathbf{0}_{W-L,L}, \mathbf{I}_{W-L,W-L}, \mathbf{0}_{W-L,L}]$. Here $\mathbf{P}\mathbf{A}^H$ is a square symmetric matrix the EVD of which is defined in the form of $\mathbf{P}\mathbf{A}^H = \mathbf{U}\mathbf{V}\mathbf{U}^H$.

$$\frac{1}{\sigma_s^2}\mathbf{R}_{\mathbf{sc}}^H \mathbf{R}_{\mathbf{sc}} = \sigma_s^2 \mathbf{P} \underbrace{\hat{\mathbf{G}}^H \hat{\mathbf{G}}}_{\mathbf{G}} \mathbf{P}^H \tag{23}$$

and

$$\mathbf{G} = \left[\begin{array}{c} \mathbf{0}_{W,W+L} \\ \hline \mathbf{0}_{L,W} | \quad \mathbf{I}_{L,L} \end{array} \right]. \tag{24}$$

Since $\mathbf{Q} = \mathbf{P} + \gamma\mathbf{A}$ and $\mathbf{P}\mathbf{G}^H = \mathbf{Q}\mathbf{G}^H$, we have

$$\begin{aligned} \mathbf{f}_F &= \sigma_s^2 \mathbf{d}_\Delta \mathbf{P}^H (\sigma_s^2 \mathbf{P}\mathbf{P}^H + \sigma_n^2 \mathbf{P}\mathbf{A}^H - \sigma_s^2 \mathbf{P}\mathbf{G}\mathbf{P}^H)^{-1} \\ &= \mathbf{d}_\Delta \mathbf{P}^H ((\mathbf{Q} - \mathbf{P}\mathbf{G}^H)\mathbf{P}^H)^{-1} \\ &= \mathbf{d}_\Delta ((\mathbf{Q} - \mathbf{Q}\mathbf{G}^H)\mathbf{P}^H \mathbf{U}\mathbf{V}^{-1}\mathbf{U}^H)^{-1} \quad (25) \\ &= \mathbf{d}_\Delta \boldsymbol{\Upsilon}^{-1} \quad (26) \end{aligned}$$

where $\mathbf{d}_\Delta$ denotes a "row" vector with all zero entries except the $(\Delta+1)$th entry to be 1(one) to ensure that the right delay is initiated at the correct position in the matrix of equation (25).

$\mathbf{P}^H$ can also be written as $\mathbf{P}^H = \hat{\mathbf{U}}\mathbf{V}\mathbf{U}^H$, where $\hat{\mathbf{U}} = \begin{bmatrix} \boldsymbol{\Gamma}_1 \\ \mathbf{U} \\ \boldsymbol{\Gamma}_2 \end{bmatrix}$. In addition to the eigenvector matrix $\mathbf{U}$, each one of $\boldsymbol{\Gamma}_1$ and $\boldsymbol{\Gamma}_2$ introduces L new row vectors, which corresponds to the top L rows, denoted by $\boldsymbol{\Pi}_1$, and bottom L rows, denoted by $\boldsymbol{\Pi}_2$, of $\mathbf{P}^H$. Therefore, $\begin{bmatrix} \boldsymbol{\Gamma}_1 \\ \boldsymbol{\Gamma}_2 \end{bmatrix} \mathbf{V}\mathbf{U}^H = \begin{bmatrix} \boldsymbol{\Pi}_1 \\ \boldsymbol{\Pi}_2 \end{bmatrix}$, so that $\begin{bmatrix} \boldsymbol{\Gamma}_1 \\ \boldsymbol{\Gamma}_2 \end{bmatrix} = \begin{bmatrix} \boldsymbol{\Pi}_1 \\ \boldsymbol{\Pi}_2 \end{bmatrix} \mathbf{U}\mathbf{V}^{-1}$, which transforms $\boldsymbol{\Upsilon}$ in (26) into

$$\boldsymbol{\Upsilon} = (\mathbf{Q} - \mathbf{Q}\mathbf{G}^H)\hat{\mathbf{U}}\mathbf{U}^H,$$

and further be simplified as

$$\begin{aligned} \boldsymbol{\Upsilon} &= \begin{bmatrix} \boldsymbol{\Pi}_1^H & \boldsymbol{\Psi} & \mathbf{0}_{J,L} \end{bmatrix} \times \begin{bmatrix} \boldsymbol{\Gamma}_1 \mathbf{U}^H \\ \mathbf{I}_{J,J} \\ \boldsymbol{\Gamma}_2 \mathbf{U}^H \end{bmatrix} \\ &= \boldsymbol{\Pi}_1^H \boldsymbol{\Pi}_1 \mathbf{U}\mathbf{V}^{-1}\mathbf{U}^H + \boldsymbol{\Psi}. \end{aligned} \tag{27}$$

where $\boldsymbol{\Psi} = \mathbf{Q}\mathbf{A}^H$.

Once $\mathbf{f}_F$ is calculated, $\mathbf{f}_B$ can be found as given in (38).

The Adaptive Estimation of the Equalizer coefficients: To obtain an estimate for the channel equalizer, in the form of (16), (10) is modified as

$$\tilde{\mathbf{f}}_C(k+1) = \tilde{\mathbf{f}}_C(k) + \chi e(k)\mathbf{r}_C^H(k). \tag{28}$$

In (28)

$$\begin{aligned} \tilde{\mathbf{f}}_C(k) &= [\tilde{\mathbf{f}}_F(k), -\tilde{\mathbf{f}}_B(k)] \\ \mathbf{r}_C(k) &= [\mathbf{r}_I^T(k), \mathbf{x}^T(k-1)]^T \\ e(k) &= s_I(k-\Delta) - x(k) \\ \mathbf{x}(k) &= [x(k),\ x(k-1), \cdots,\ x(k-L+1)]^T, \end{aligned}$$

where

$$x(k) = \tilde{\mathbf{f}}_C(k) \times \mathbf{r}_C(k) \tag{29}$$

and the equalization delay is as in (20). The equation in (28) estimates $\tilde{\mathbf{f}}_F$ and $\tilde{\mathbf{f}}_B$ to realize the system in (16). As explained earlier, it is expected that the LMS algorithm converges around the optimum channel equalizer, i.e. $F(z) = 1/Q(z)$, which can be decomposed into feedforward and feedback components as $F_F(z) = 1/(\theta_0 \bar{T}(z))$ and $F_B(z) = T(z)$ making use of the spectral factorization of $Q(z)$ [31, $page$ 199] stating that $Q(z) = \theta_0 \bar{T}(z) T(z)$.

$T(z) = \sum_{i=0}^{L} t(i) z^{-i}$ is causal, minimum phase filter while $t(0) = 1$ and θ_0 is a positive real number, which guarantees $F_B(z)$ being in FIR structure as mandated by the conventional BMF receiver design. To realize an FIR feedforward filter too, instead of $F_F(z) = 1/(\theta_0 \bar{T}(z))$, the Δth vector from $\theta_0 \mathbf{T}$'s pseudoinverse matrix can be selected as follows

$$\begin{aligned} \tilde{\mathbf{f}}_F &= \mathbf{d}_\Delta (\theta_0 \mathbf{T})^\dagger \\ &= \mathbf{d}_\Delta \theta_0 \mathbf{T}^H ({\theta_0}^2 \mathbf{T}\mathbf{T}^H)^{-1} = \mathbf{d}_\Delta \boldsymbol{\Psi}^{-1}. \end{aligned} \tag{30}$$

where $\mathbf{T} = \mathcal{C}onv(\bar{T}(z))$ and Δ is as in (20). $(\cdot)^\dagger$ represents Moore-Penrose pseudoinverse.

Here we can conclude that, the feedforward filter that the LMS algorithm in (28) estimates can be approximated with (30).

Effect of the Feedforward Filter length: Because $\boldsymbol{\Pi}_1^H \boldsymbol{\Pi}_1$ is composed of zeros except its $L\times L$ leading principal minor, the term $\boldsymbol{\Pi}_1^H \boldsymbol{\Pi}_1 \mathbf{U}\mathbf{V}^{-1}\mathbf{U}^H$ in (27) would only be effective over the first L rows of $\boldsymbol{\Upsilon}$. This in fact corresponds to a transient response, which can be ignored if the length of the channel equalizer is significantly larger than the channel length (e.g. $J \geq 5L$ [1]) for the selected delay $\Delta = J + L - 1$. Therefore, when J is selected long enough, both $\mathbf{d}_\triangle \mathbf{\Upsilon}^{-1}$ in (26) and $\mathbf{d}_\triangle \mathbf{\Psi}^{-1}$ in (30) will lead to approximately the same result.

In Appendix B it is shown that as J gets larger, the very last coefficient of $\mathbf{f}_F$ increases in value, while that of early filter coefficients get smaller and reach to zero. Since the first L components would be equal to zero, the filter in (30) can also be used as an alternative to (26).

We can conclude that the optimum IIR equalizer for the communication channel of (9) can also be used to equalize the channel depicted in the conventional BMF design by selecting the equalizer length long enough. Supportive simulation results will be provided in the next section.

C. Algorithm Summary

Our novel all-adaptive blind matched filter approach can be summarized as follows

Step-1) Using (8), obtain an estimate for $Q(z)$.

Step-2) Setup (9) to obtain $\mathbf{r}_I(k)$.

Step-3) Run the recursive algorithm (10) to obtain $\tilde{\mathbf{f}}$ (or run (28) and obtain $\tilde{\mathbf{f}}_F$ and $\tilde{\mathbf{f}}_B$).

Step-4) Setup the receiver in Fig.1(b) and obtain $x(k)$ via (13) or via (29).

Step-5) CMA, given in (12), converges to the unknown channel matched filter, which is simply the time reversed conjugate (paraconjugate) of the channel itself.

$Remark$ 1) Although it is summarized as an approach with 5 consecutive steps, all of these steps can run concurrently. Therefore, there is no need to wait for one step to be accomplished in order to go for the next one. In the simulations section we will provide a simulation result, where all five steps run simultaneously (in parallel) , which doesn't affect the performance of the BMF receiver at all.

$Remark$ 2) It should also be noted that Step-1, Step-4 and Step-5 are kept almost the same as they are in the conventional BMF receiver. The only two differences are; The need for the estimation of σ_n^2 was discarded in Step-1, and for the calculation of the channel equalizer, needed to implement Step-4, no matrix operations such as inversion and multiplication were used with the help of Step-2 and Step-3.

All-adaptive BMF receiver for Fractionally Spaced Equalization: The matched filter receiver depicted in Fig.1(a) is in the same form as the Forney's matched filter receiver [3]. However, the receiver in [3] needs for an analog matched filter and the matched filter in our design is a baud spaced FIR filter.

On the other hand, Fractionally Spaced Equalization (FSE) is regarded as an alternative to the use of analog matched filters at the front-end [25]. Here in this section we will talk about all-adaptive BMF receiver if it is intended to be operated on the oversampled signals required to perform FSE.

In theory the FSE and the communications over Single Input Multiple Output (SIMO) channels behave similarly. Therefore, in this part we will make use of the findings from [11], which describes BMF receivers for SIMO communications.

Based on [11], the use of all-adaptive design on oversampled signals requires for two modifications

1) If B is the oversampling rate, in order to realize the AFA-AR filter in Fig.2, $\tilde{\mathbf{q}}$ should be calculated by setting

$$\tilde{\mathbf{q}} = \sum_{b=1}^{B} \tilde{\mathbf{q}}_b, \tag{31}$$

where $\tilde{\mathbf{q}}_b$ represents the vector of auto-correlation estimate for the bth fraction of oversampled signal.

2) Set

$$\mathbf{x}(k) = [x_1(k),\ x_1(k-1)..., x_1(k-L), x_2(k), \\ ...\ x_B(k-L)], \tag{32}$$

in (12), where

$$x_b(k) = \mathbf{f} \times \mathbf{r}_b(k), \quad \text{for} \quad b = 1, ..., B. \tag{33}$$

In (33) $\mathbf{r}_b(k)$ is the channel output for the bth fraction. Note that same channel equalizer $\mathbf{f}$ is used to filter each $\mathbf{r}_b(k)$ for $b = 1, ..., B$. $\mathbf{f}$ is estimated from the AFA-AR filter, shown in Fig.2, by setting $\tilde{\mathbf{q}}$ as in (31). The result of (12) will include the matched filter components corresponding to each part as follows

$$\tilde{\mathbf{m}}(k) = [\tilde{\mathbf{m}}_1(k),\ \tilde{\mathbf{m}}_2(k), ..., \tilde{\mathbf{m}}_B(k)], \tag{34}$$

Apart from the two modifications listed in the above two paragraphs, the Forney's matched filter receiver operates along the Viterbi Algorithm, which is a nonlinear solution to the equalization of the communication channels. Due to nonlinearity the use of the Viterbi algorithm would not be possible with the all-adaptive design. However, once the matched filter is estimated so that the channel is, the channel estimate could be used to perform the Viterbi algorithm while the channel being updated in decision directed mode. See [26] for further reading on how the Viterbi algorithm can be used in the BMF receivers.

We can conclude that, although there is not a one-to-one relationship between the all-adaptive matched filtering and the Forney's matched filter, some modifications are possible to enhance the equalization performance of our receiver to get closer to that of Forney's matched filter receiver.

Architectural Complexity: The highest complexity in the AFA-AR filter, depicted in Fig.2, is at the implementation of the LMS algorithm. $2J{+}1$ multiplications and $2J$ additions are required to implement the LMS algorithm at each iteration formulated in (10). The circuitry to create $\mathbf{r}_I(k)$, formulated in (9) is only a FIR filter with complexity of $L{+}1$ multiplications and $2L$ additions. The least computationally complex component of the AFA-AR filter is the binary random sequence generator that creates $\mathbf{s}_I(k)$. Random number generators are a good choice due to their circuits being simple to be implemented [28]. Two clock signals, running in frequencies that are not

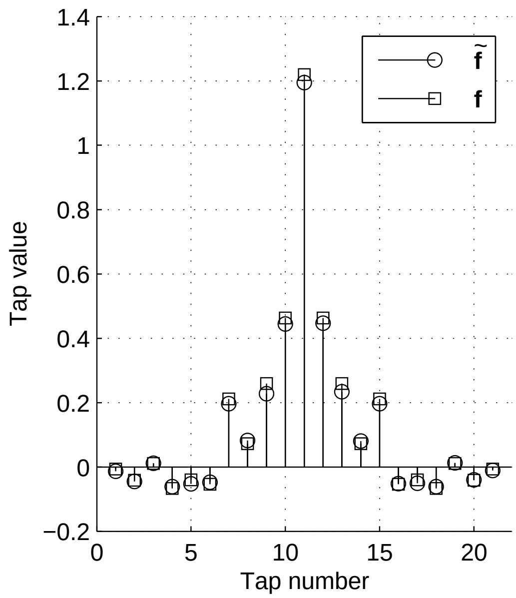

Fig. 3. The tap values for $\mathbf{f}$ and $\tilde{\mathbf{f}}$ if $\tilde{\mathbf{q}}$ is estimated

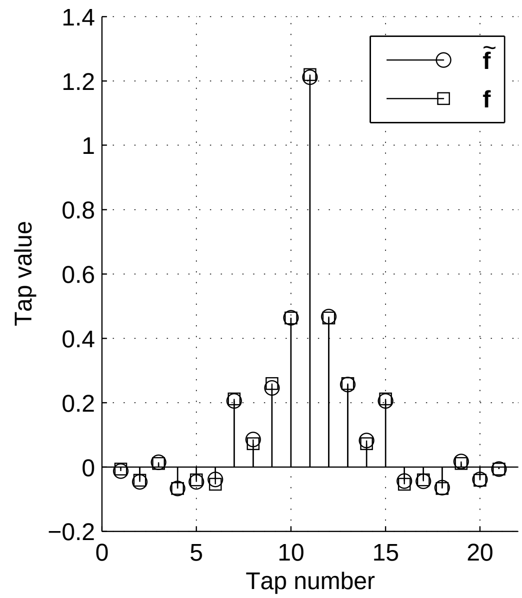

Fig. 5. The tap values for $\mathbf{f}$ and $\tilde{\mathbf{f}}$ if true $\mathbf{q}$ values are used.

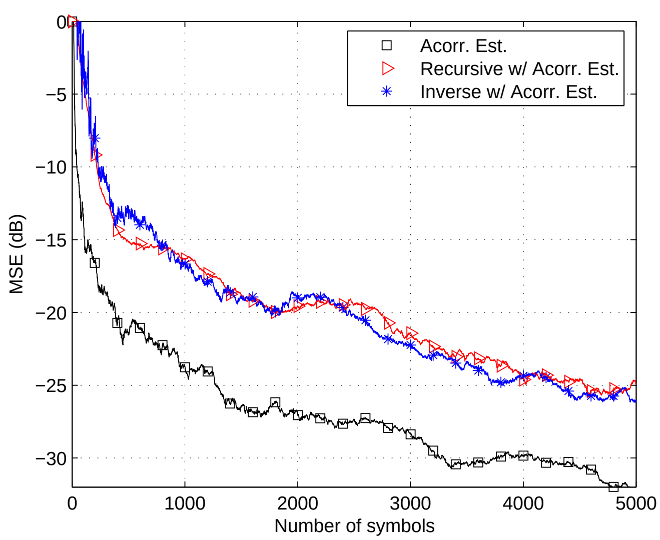

Fig. 4. MSE performance of the estimates, found for the two layer FIR filter given in Fig.2 if $\tilde{\mathbf{q}}$ is estimated.

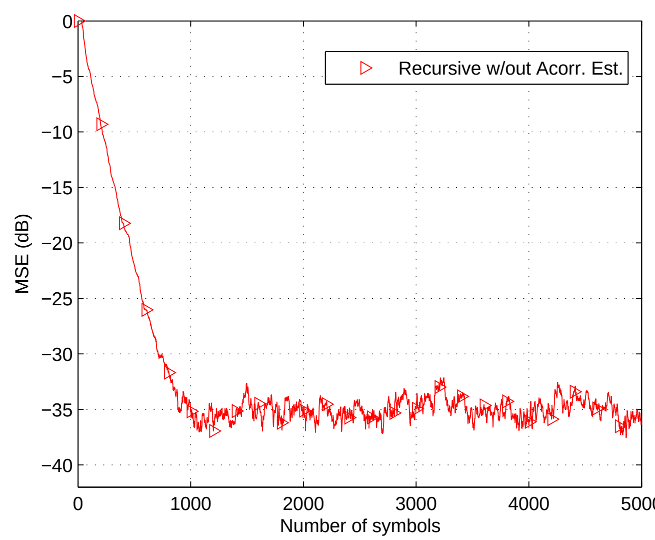

Fig. 6. MSE performance of the estimates, found for the two layer FIR filter given in Fig.2. if true $\mathbf{q}$ values are used.

multiples of each other, connected to comparator would be an efficient solution for creating a random binary sequence. On the other hand Linear-Feedback Shift Registers (LFSR) are commonly used to create pseudo random sequences, where the complexity is a number of Flip Flops (FFs) and XOR gates. For example, to create a pseudo random binary sequence that repeats itself after $2^{10} - 1$ samples, a circuitry of 10 FFs and 2 XOR gates are enough [29].

Apart from the AFA-AR filter, the all-adaptive BMF receiver needs for the CMA and the sample averaging circuit both inheriting from the conventional BMF design. Therefore the total number of multipliers and the adders to realize the all-adaptive BMF receiver is $3J + 5L + 9$ and $3J + 5L + 2$ respectively plus the pseudo-random number generator. Because $J \gg L$, almost half of the anticipated architecture has been occupied by the LMS algorithm. In comparison to algorithms where matrix inversion and noise variance estimates are needed for channel equalization (such as [19] and [1]) or the ones using matrix decomposition rules (like [4]–[10]), the use of our novel receiver is computationally promising with a complexity order of $\mathcal{O}(J, L)$.

IV. Simulations

We will present two sets of simulations in this section. In the first set of simulations the convergence of the AFA-AR filter and its tracking capability in time varying channels will be tested. In the second set, the channel identification and equalization performance of the all-adaptive BMF will be compared with the conventional BMF design and two other methods from the literature.

For the simulations, unit energy BPSK symbol transmission is assumed from a single transmit antenna to a single receive antenna. We assume a discrete FIR communication channel where the channel memory size is already known by the receiver. The noise added to the received signals is assumed to be white and Gaussian distributed (i.e., AWGN), and the noise variance is not known to the receiver. To enable the repeatability of the simulations here we define two CIRs both of order $L = 5$, $\mathbf{h}_{min} = -0.722 + 0.567z^{-1} + 0.081z^{-2} - 0.107z^{-3} + 0.254z^{-4} - 0.274z^{-5}$, which is a minimum phase channel and $\mathbf{h}_{mix} = -0.362 + 0.159z^{-1} + 0.524z^{-2} + 0.268z^{-3} + 0.458z^{-4} - 0.536z^{-5}$, which is a mixed phase channel.

A. AFA-AR filter

In the conventional BMF design, the tap values of the equalizer can only be calculated if the process for the auto-correlation function estimation is finalized. In our novel design we aim to run the AFA-AR filter in parallel with the auto-correlation estimation process, formulated in (8), which also enables the tracking capability of changes in the CIR. In this first set of simulations we reveal how good the AFA-AR filter performs the calculation of the true channel equalizer parameters during the channel auto-correlation estimation takes place.

For simulations, the correct equalizer filter coefficients vector is calculated as in (30). However, because the use of feedback filter is not needed, there is no constraint on the choice of Δ. Fig.3 compares the correct equalizer filter tap values of $\mathbf{f}$ (using true $\mathbf{q}$) with $\tilde{\mathbf{f}}$, estimated iteratively as shown in (10) using the estimate $\tilde{\mathbf{q}}$. The difference between the two filters was found to be around -25 dB, where the difference is defined in Mean Squared Error (MSE) sense averaging $||\tilde{\mathbf{f}} - \mathbf{f}||^2 / ||\mathbf{f}||^2$. Please note that only $\mathbf{h}_{min}$ was used to create simulation results from Fig.3 to Fig.6.

Three results are shown in Fig.4. '$Acorr.Est$' shows the MSE for the auto-correlation function estimation. '$Recursive\ w/Acorr.Est$' is the MSE, incurred in converging to the true $\mathbf{f}$, if AFA-AR filter is preferred. '$Inverse\ w/Acorr.Est$' is the MSE result in the same sense if matrix inversion is preferred as in (30). Note that the tap values $\tilde{\mathbf{f}}$ in Fig.3 are the result of '$Recursive\ w/Acorr.Est$'. From Fig.4 it is clear that the MSE made by the AFA-AR filter decreases along with the decrease in the estimation error for the auto-correlation function. Another outcome of Fig.4 is that, there is almost no performance loss if matrix inversion is replaced with the AFA-AR filter.

Similar to Fig.3, Fig.5 compares $\mathbf{f}$ with $\tilde{\mathbf{f}}$ again but this time $\tilde{\mathbf{f}}$ is estimated by using the true auto-correlation function of the channel output, i.e. $\mathbf{q}$ rather than $\tilde{\mathbf{q}}$. The MSE drops down to -35 dB this time, showing that the tap values of $\tilde{\mathbf{f}}$ were found to be almost equal to those of $\mathbf{f}$, which can easily be realized comparing Fig.3 and Fig.5. Fig.6 was created similarly to Fig.4 but this time it was assumed that $\mathbf{q}$ was perfectly known. The plot '$Acorr.Est$' is no longer needed and because '$Inverse\ w/Acorr.Est$' will calculate $\mathbf{f}$ perfectly, it is also not needed to be included in Fig.6. It is clear that the MSE is lowered by another $10dB$ and the AFA-AR filter performed a better estimate of $\mathbf{f}$ in comparison to Fig.4.

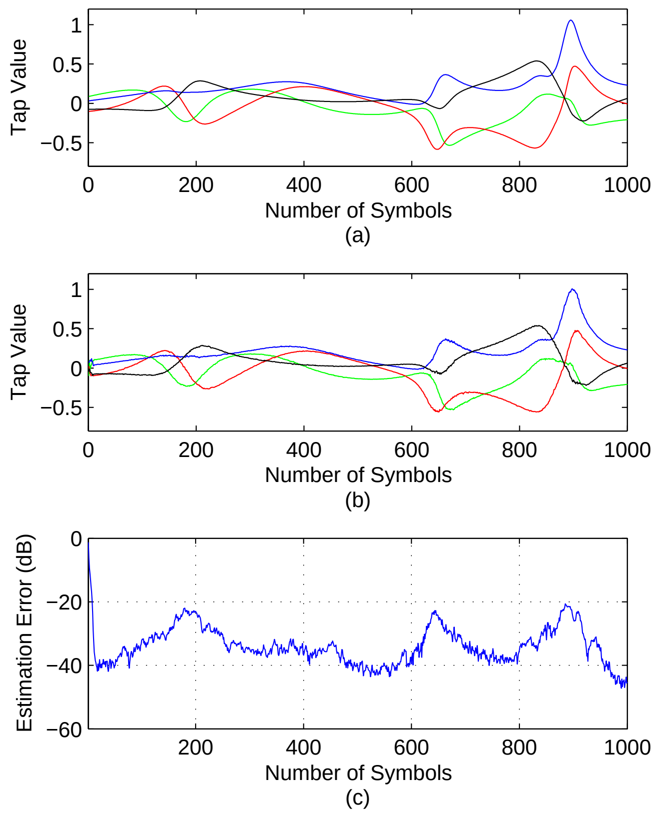

Fig. 7. The tracking capability of the AFA-AR filter, when the channel is time varying.

The plots in Fig.3 to Fig.6 show that the AFA-AR filter estimates the true equalizer almost perfectly. The MSE performance of the convergence of the adaptive filter relies vastly on how good the auto-correlation function is estimated. As the estimation error of the auto-correlation function is inherited from the conventional BMF design, we can here conclude that replacing matrix inversion with the adaptive filter, proposed in Section III, does not cause a performance loss in finding $\mathbf{f}$.

In Fig.7 the tracking capability of the AFA-AR filter when deployed in the ITU Vehicular B Channel [30] was tested using MATLAB^{TM}'s `rayleighchan` command with 2 GHz carrier frequency, 40 km/hr velocity and 400 kbps transmission rate. Simulation parameters are set to $\chi = 0.02$, $J = 31$. Fig.7 includes three subplots. Fig.7(a) shows how two of the equalizer coefficients are varying in time. Because both of these coefficients are formed of an imaginary and a real part, in total of 4 plots are given in Fig.7(a). Fig.7(b) shows the same two coefficients estimated by the AFA-AR filter. Fig.7(a) and Fig.7(b) are identical which shows which shows how good the AFA-AR filter tracks the changes in a time-varying channel. Fig.7(c) simply gives the estimation error calculated as $||\tilde{\mathbf{f}} - \mathbf{f}||^2 / ||\mathbf{f}||^2$. Although in some channel conditions the

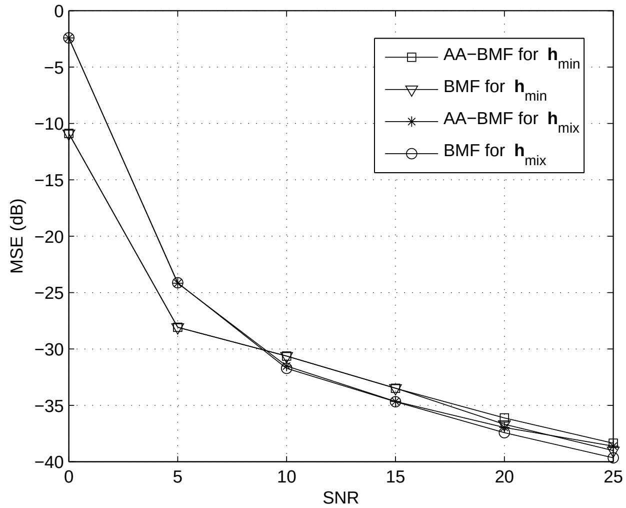

Fig. 8. MSE performance of the channel impulse response estimation in both the BMF receiver and its all-adaptive design as SNR increases.

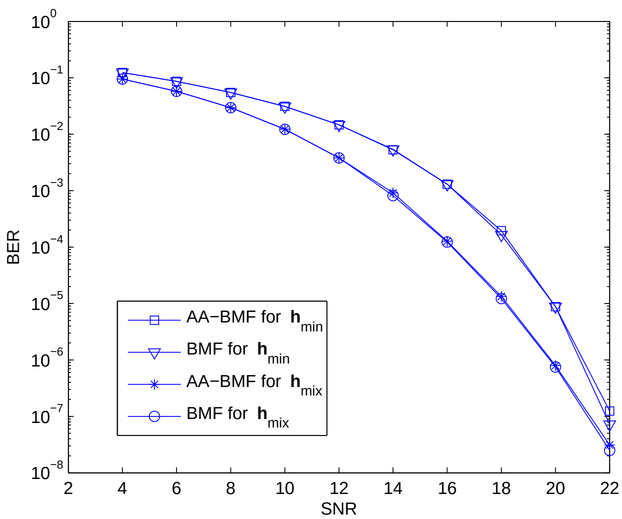

Fig. 9. BER performance of both the BMF receiver and its all-adaptive design

estimation performance of the AFA-AR filter drops, almost all the times the estimation error stays below $-20dB$. Note that Fig.7 is the result of a single simulation rather than an average of a number of runs.

B. Performance of the All-Adaptive BMF Receiver

In Fig.8 two sets of plots are shown. Fig.8 compares the MSE performance of the CIR estimation for the conventional and the all-adaptive designs as the SNR increases for both of the channels, $\mathbf{h}_{min}$ and $\mathbf{h}_{mix}$. Note that for the update of all-adaptive design, equation given in (28) was used. The simulation parameters for the CMA algorithm were selected as; $J = 31$, $\mu = 0.015$ for $\mathbf{h}_{min}$ and $\mu = 0.02$ for $\mathbf{h}_{mix}$. In Fig.8 '$AA - BMF$' corresponds to the all-adaptive BMF and 'BMF' is the conventional BMF. Fig.8 clearly shows that both of the receivers, all-adaptive BMF and the conventional BMF, performed at almost the same convergence rate for both mixed phase and minimum phase channels.

In Fig.9 the Bit Error Rate (BER) performance of the two receivers were shown for selected SNR levels. For these simulations the communication channel was assumed to be known by the receiver as to realize the equalization performance apart from the blind channel estimation process. It is clear from Fig.9 that the BER performance of the conventional BMF receiver and the all-adaptive BMF are almost the same. The minuscule difference can be attributed to the non-vanishing step-size of the LMS algorithm. It should be noted that the BER performance varies if a different channel was selected. We can here conclude that the performance of the all-adaptive BMF is the same with the conventional BMF receiver and can be used as an alternative to the BMF receiver. Therefore, there would be no noteworthy loss in the equalization performance if the all-adaptive approach is preferred.

The performance of the CMA degrades if it is used to recover non-constant modulus signals. In Fig.10 we have simulated the channel estimation performance of the all-adaptive BMF receiver when signal modulation scheme is 16-QAM, where the estimation errors from 100 consecutive simulations were averaged. The SNR is 7 dB and the communication channel is the oversampled channel $h(t)$ from $[19, page\ 1384]$, where the communication channel and the AWGN are composed of complex numbers. In order to compare its performance with other methods from the literature, the FSE is performed in all-adaptive BMF receiver as explained in Section III.C. In Fig.10 '$SS - Method$' is the error made with the well known subspace method from [4]. '$Rec - AS$' is the method in [19].

The '$AA - BMF(CMA)$' shows the channel estimation performance of the all-adaptive BMF receiver. On the other hand '$AA-BMF(MMA)$' is that of performance if equation (12) is replaced with the Multi Modulus Algorithm (MMA) [27]. The MMA equation we have replaced (12) with is as follows

$$\tilde{\mathbf{m}}(k) = \tilde{\mathbf{m}}(k-1) - \mu((Re\{y(k)\}^2 - R_{2,R})Re\{y(k)\} \\ +j(Im\{y(k)\}^2 - R_{2,I})Im\{y(k)\})\mathbf{x}^H(k) \quad (35)$$

where $R_{2,R}$ and $R_{2,I}$ are the dispersion constants with respect to the real and imaginary axis respectively. For the 16-QAM constellation $R_{2,R} = R_{2,I} = 0.82$. In (35), $Re\{y(k)\}$ and $Im\{y(k)\}$ are the real and imaginary parts of of $y(k)$ and $j = \sqrt{-1}$. When creating Fig.10 we set $\mu = 0.02$ but changed it to $\mu = 0.005$ at the 5000th sample.

The use of the MMA has improved the channel estimation performance of the all-adaptive BMF as it was originally designed to work well with non-constant modulus signals too. On the other hand, our novel receiver performs channel estimation almost as good as other methods from the state-of-the-art, which are relatively more computationally complex.

V. CONCLUSION

In this paper, we have presented a practical approach, called "all-adaptive blind matched filtering", which replaces

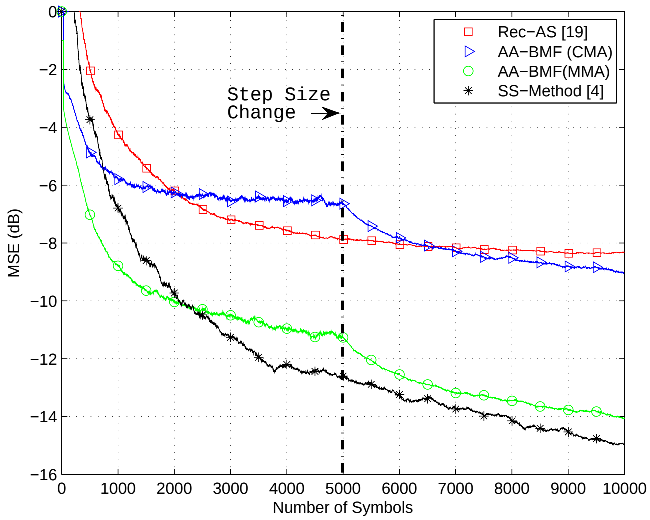

Fig. 10. MSE performance of the all-adaptive BMF receiver using CMA and MMA,

the conventional BMF receiver. In the novel design the matrix inversion and matrix multiplication operations were replaced with a simple recursive algorithm. Therefore, the proposed all-adaptive approach brings simplicity to the implementation of blind matched filtering. It has been shown through our simulations section that the performance of the recursive algorithm is almost the same as the performance of its matrix inversion counterpart. The recursive method runs in parallel to the channel auto-correlation estimation process, where this process is also a must in the conventional design. The recursive algorithm has also enabled the tracking capability of any change in the channel auto-correlation estimate. Another benefit of using the all-adaptive approach is that the calculation of the MMSE equalizer no longer needs the noise variance estimation. The calculation of the MMSE equalizer filter was performed solely on the channel auto-correlation estimate. The channel identification and equalization performance of our novel receiver was compared to the conventional BMF receiver and it was observed that they achieved almost equal MSE and BER levels, for the same experimental conditions and parameters at a much reduced computational burden.

We also would like to state that the implementation of the so called AFA-AR filter is simply represented as a random training sequence generator with an adaptive filter being updated via LMS in this paper. This representation is useful to understand the concept that we aim to introduce for the realization of the all-adaptive BMF receiver. However, when it comes down to the implementation of the AFA-AR filter in a real-life hardware platform or an integrated chip solution further details of the actual implementation and their possible constraints should be given. These aspect will be reported in a future upcoming paper.

Appendix A
Conventional Blind Matched Filter Receiver

For the conventional BMF receiver the feedforward filter $\mathbf{f}_F$ is calculated solving the following equation [1], modified to comply with our notations and assumptions in this paper;

$$\begin{bmatrix} \beta(-J+1,-J+1) & \cdots & \beta(-J+1,0) \\ \vdots & \ddots & \vdots \\ \beta(0,-J+1) & \cdots & \beta(0,0) \end{bmatrix} \times \begin{bmatrix} f_F(0) \\ \vdots \\ f_F(J-1) \end{bmatrix} = \begin{bmatrix} q(-J+1) \\ \vdots \\ q(0) \end{bmatrix}, \quad (36)$$

where

$$\beta(i,j) = \sum_{l=-L}^{-j} q(l)q^*(l+j-i) + \gamma q(i-j) \quad (37)$$

for $i,j = -J+1,...,0$. The feedback filter, $\mathbf{f}_B = [\ f_B(1), \ \cdots, \ f_B(L)\ ]$ of length L is found by

$$f_B(i) = \sum_{l=i-L}^{0} f_F(l+J-1)q(i-l) \qquad \text{for} \ \ i = 1,...,L. \quad (38)$$

Appendix B
Feedforward Filter Coefficients of the IIR BMF Receiver

$\mathbf{\Psi}$ is a Toeplitz positive definite matrix (See Appendix C) of size $J\times J$. We define a new matrix $\widehat{\mathbf{\Psi}}$ of size $(J-1)\times(J-1)$, which is formed by removing the last row and column of $\mathbf{\Psi}$. Therefore, $\widehat{\mathbf{\Psi}}$ is also a Toeplitz positive definite matrix.

Define a vector $\mathbf{g} = \mathbf{d}_{\triangle}\mathbf{\Psi}^{-1}$ where $\mathbf{g} = [g(0), g(1), ..., g(J-1)]$. Using cofactors of $\mathbf{\Psi}$

$$|g(0)| = \frac{|\zeta_{J,1}|}{det(\mathbf{\Psi})} \quad \text{and} \quad |g(J-1)| = \frac{\zeta_{J,J}}{det(\mathbf{\Psi})} \quad (39)$$

for the first and the last elements of $\mathbf{g}$ respectively, where $det(\cdot)$ represents determinant and the $\zeta_{i,j}$ is the cofactor corresponding to the ith row and jth column of $\mathbf{\Psi}$. $|\cdot|$ operator takes the magnitude of the scalar it contains.

For the Toeplitz positive definite matrix $\mathbf{\Psi}$,

$$\lim_{J\to\infty} \frac{\zeta_{J,J}}{det(\mathbf{\Psi})} = \lim_{J\to\infty} \frac{1}{det(\mathbf{\Psi})^{\frac{1}{J}}}, \quad (40)$$

where the term $\frac{\zeta_{J,J}}{det(\mathbf{\Psi})}$ is increasing as J increases [33]. For a J, when equality in (40) holds regardless of the limit operator, $g(J-1)$ will be constant as J increases and $\zeta_{J,J}$ will increase or decrease with a constant rate $\tau_{J,J} = 1/g(J-1)$ if the equalizer size is increased by 1. Therefore, $\tau_{J,J}.det(\widehat{\mathbf{\Psi}}) = det(\mathbf{\Psi})$.

Calling the the cofactors of $\widehat{\mathbf{\Psi}}$, $\widehat{\zeta}_{i,j}$,

$$\zeta_{J,1} = q(0).\widehat{\zeta}_{J,J} + q(1).\widehat{\zeta}_{J-1,J} + ... + q(J-1).\widehat{\zeta}_{1,J}, \quad (41)$$
$$\zeta_{J,J} = q(J-1).\widehat{\zeta}_{J,J} + q(J-2).\widehat{\zeta}_{J-1,J} + ... + q(0).\widehat{\zeta}_{1,J}.$$

As can be seen in (41), $\zeta_{J,1}$ and $\zeta_{J,J}$ are composed of the same cofactors. Because $q(i)$ for $i = 0, ..., J-1$ are constant, $\tau_{J,1} \neq \tau_{J,J}$, where $\tau_{J,1}$ is the rate of change for $\zeta_{J,1}$ as equalizer size increases. As the possibility where $\tau_{J,1} > \tau_{J,J}$ is contrary to the applicability of the equalization, then $\tau_{J,1} < \tau_{J,J}$. Therefore, we can conclude that the value of the newly added coefficients as J increases are decreasing due to (39).

APPENDIX C
STRUCTURE OF $\mathbf{\Psi}$

$\mathbf{PA}^H$ can also be formulated as $\mathbf{PA}^H = \mathbf{H}^H\mathbf{H}$, which is actually the channel autocorrelation matrix. $\mathbf{H}^H\mathbf{H}$ is positive semi-definite matrix [32], its eigenvalues $v_1, v_2, ..., v_J$ being $v_i \geq 0$ for $i = 1, ..., J$. As $\mathbf{\Psi} = (\mathbf{P} + \gamma\mathbf{A})\mathbf{A}^H = \mathbf{PA}^H + \gamma\mathbf{AA}^H = \mathbf{PA}^H + \gamma\mathbf{I}_{J,J}$, the eigenvalues of $\mathbf{\Psi}$ are

$$v_i + \gamma > 0 \quad \text{for} \quad i = 1, ..., J \quad (42)$$

assuming that $1/\gamma \neq \infty$. Therefore, $\mathbf{\Psi}$ is a positive definite matrix in the following form,

$$\mathbf{\Psi} = \begin{bmatrix} q(0) & \cdots & q(L) & 0 & \cdots & 0 \\ q(-1) & q(0) & \cdots & q(L) & & \vdots \\ \vdots & & \ddots & \ddots & \ddots & 0 \\ \vdots & & q(-L) & \cdots & q(0) & q(1) \\ 0 & \cdots & 0 & q(-L) & \cdots & q(0) \end{bmatrix}. \quad (43)$$

It is clear from (43) that $\mathbf{\Psi}$ is also a Toeplitz matrix.

REFERENCES

[1] B. Baykal, "Blind Matched Filter Receiver", *IEEE Trans. Circuits Syst. I*, vol. 51, no.2, pp. 379 – 390, Feb. 2004.
[2] I. Ozcelik, B. Baykal and I. Kale "Blind adaptation of a matched filter using the constant modulus algorithm coupled with an optional correction method," in IEEE ISSPA'03, vol. 2, pp. 291–294, July 2003.
[3] G. D. Forney Jr., "Maximum-likelihood sequence estimation of digital sequences in presence of intersymbol interference," *IEEE Trans. Inform. Theory*, vol. IT-18, pp. 363–378, May 1972.
[4] L. Tong, G. Xu, and T. Kailath, "Blind identification and equalization based on second-order statistics: A time domain approach," *IEEE Trans. Inf. Theory*, vol. 40, no. 2, pp. 340–349, Mar. 1994.
[5] K. I. Diamantaras, and T. Papadimitriou, "An Efficient Subspace Method for the Blind Identification of Multichannel FIR Systems," *IEEE Trans. Circuits Syst. I*, vol. 56, no. 12, pp. 5833-5839, Dec. 2008.
[6] E. Moulines, P. Duhamel, J.-F. Cardoso, and S. Mayrargue, "Subspace methods for the blind identification of multichannel FIR filters," *IEEE Trans. Signal Process.*, vol. 43, no. 2, pp. 516–525, Feb. 1995.
[7] G. Xu, H. Liu, L. Tong, and T. Kailath, "A least-squares approach to blind channel identification," *IEEE Trans. Signal Process.*, vol. 43, no. 12, pp. 2982–2993, Dec. 1995.
[8] O. Grellier, P. Comon, B. Mourrain, and P. Trbuchet, "Analytical Blind Channel Identification," *IEEE Trans. Signal Process.*, vol. 50, no. 9, pp. 2196–2207, Sep. 2002.
[9] J.K. Tugnait, "Blind equalization and estimation of FIR communications channels using fractional sampling," *IEEE Trans. Commun.*, vol. 44, no. 3, pp. 324–336, Mar. 1996.
[10] J. Fang, A. R. Leyman, Y. H. Chew, and Y. C. Liang, "A Cumulant Interference Subspace Cancellation Method for Blind SISO Channel Estimation," *IEEE Trans. Signal Process.*, vol. 54, no. 2, pp.784–790, Feb. 2006.
[11] A. Coskun and I.Kale, "Blind multidimensional matched filtering techniques for single input multiple output communications," *IEEE Trans. on Instr. Meas.*, vol. 59, no. 5, pp. 1056 – 1064, May 2010.
[12] B. Baykal,"Blind channel estimation via combining autocorrelation and phase estimation," *IEEE Trans. on Circuits and Syst. I*, vol. 51, no. 6, pp. 1125–1131, June 2004.
[13] C.Y. Chi, C.Y. Chen, C.H. Chen, and C.C. Feng, "Batch processing algorithms for blind equalization using higher-order statistics," *IEEE Signal Processing Mag.*, vol. 20, pp. 25–49, Jan. 2003.
[14] J. K. Tugnait, L. Tong, and Z. Ding, "Single-user channel estimation and equalization," *IEEE Signal Process. Mag.*, vol. 17, no. 3, pp. 17-28, May 2000.
[15] F. Wan, W. Zhu, and M. N. S. Swamy, "A Signal-Perturbation-Free Transmit Scheme for MIMO-OFDM Channel Estimation," *IEEE Trans. Circuits Syst. I*, vol. 57, no. 8, pp. 2208-2220, Aug. 2010.
[16] C. Tu and B. Champagne, "Subspace-Based Blind Channel Estimation for MIMO-OFDM Systems With Reduced Time Averaging," *IEEE Trans. Vehic. Tech.*, vol. 59, no. 3, pp.1539–1544, Mar. 2010.
[17] H. Cheng and S. C. Chan, "Blind Linear MMSE Receivers for MC-CDMA Systems," *IEEE Trans. Circuits Syst. I*, vol. 54, no. 2, pp. 367-376, Feb. 2007.
[18] Y. Chen and C. Lin, "Blind-Channel Identification for MIMO Single-Carrier Zero-Padding Block-Transmission Systems," *IEEE Trans. Circuits Syst. I*, vol. 55, no. 6, pp. 1571-1579, Jul. 2007.
[19] M. S. Radenkovic and T. Bose, "A Recursive Blind Adaptive Identification Algorithm and Its Almost Sure Convergence", *IEEE Trans. Circuits and Syst. I*, vol. 54, no.6, pp. 1380 – 1388, Feb. 2007.
[20] L. Ma, K. Dickson, J. McAllister, and J. McCanny, " QR decomposition-based matrix inversion for high performance embedded MIMO receivers," *IEEE Trans. Signal Process.*, vol. 59, no. 4, pp. 1858–1867, April 2011.
[21] D. Godard, "Self-recovering equalization and carrier tracking in two-dimensional data communication systems," *IEEE Trans. Commun.*, vol. COM-28, no. 11, pp. 1867–1875, Nov. 1980.
[22] C. R. Johnson, Jr., P. Schniter, I. Fijalkow, L. Tong, J. D. Behm, M. G. Larimore, D. R. Brown, R. A. Casas, T. J. Endres, S. Lamborathan, A. Touzni, H. H. Zeng, M. Green, and J. R. Treichler, "The core of FSE-CMA behavior theory," in *Unsupervised Adaptive Filtering*, vol. 2, *Blind Deconvolution*, S. Haykin, Ed. New York: Wiley, 2000.
[23] H. Zeng, L. Tong, and C. Johnson, "Relationships between the constant modulus and Wiener receivers," *IEEE Trans. Inf. Theory*, vol. 44, no. 4, pp. 1523-1538, Jul. 1998.
[24] P. Schniter and C. R. Johnson Jr, "Bounds for the MSE performance of constant modulus estimators," *IEEE Trans. Inform. Theory*, vol. 46, no.7, pp. 2544–2560, Nov. 2000.
[25] D. K. Borah, R. A. Kennedy, Z. Ding, and I. Fijalkow, "Sampling and prefiltering effects on blind equalizer design," *IEEE Trans. Signal Processing*, vol. 49, pp. 209-218, Jan. 2001.
[26] I. Ozcelik, B. Baykal and I. Kale "Decision feedback equalizer with the blind matched filter estimation," in IEEE ISCAS'05, vol. 6, pp. 5746–5749, May 2005.
[27] J. Yang, J.-J. Werner, and G. Dumont, "The multimodulus blind equalization and its generalized algorithms," *IEEE J. Sel. Areas Commun.*, vol. 20, no. 5, pp. 997-1015, June 2002.
[28] C. S. Petrie and J. A. Connelly, "A noise-based IC random number generator for applications in cryptography," *IEEE Trans. Circuits Syst. I, Fundam. Theory Appl.*, vol. 47, no. 5, pp. 615–621, May 2000.
[29] Alfke, P., "Efficient Shift Registers, LFSR Counters, and Long Pseudo Random Sequence Generators," *Xilinx application note*, version 1.1, Jul 1996.
[30] ITU-R Rec. M 1225, "Guidelines for evaluation of radio transmission technologies for IMT-2000," 1997.
[31] J. Cioffi, *EE379A Digital Communications: Signal Processing Class 654 reader*, Stanford University, Stanford, CA, 2008.
[32] Y. Wang and X. Dong, "Frequency-domain channel estimation for SCFDE in UWB communications," in *IEEE Trans. Commun.*, vol. 54, no. 12, pp. 2155–2163, Dec. 2006.
[33] T. Cover and J. Thomas, *Elements of Information Theory*. New York: Wiley, 1991.

Adem Coskun received the B.Eng. degree (with First class honors) in Telecommunications and Computer Networks Engineering from London South Bank University, London, U.K., in 2003, the B.Sc. degree in Electronics Engineering (Double Major in Computer Engineering) from F.M.V. Isik University, Istanbul, Turkey, in 2004, the M.Sc. degree in Electrical and Electronics Engineering from the Middle East Technical University, Ankara, Turkey, in 2007 and Ph.D. degree in blind channel identification for wireless communications from University of Westminster, London, U.K., in 2011.

He worked as a Patent Examiner in the Turkish Patent Institute (TPE) and as a member of the Standards Preparation Committee in the Turkish Standards Institute (TSE). His is currently a Research Fellow at the Applied DSP and VLSI Research Group (ADVRG), University of Westminster. His research interests include space-time wireless communications, Orthogonal Frequency Division Multiplexing (OFDM), Global Navigation Satellite Systems (GNSS) and Efficient Techniques for On-Board Processing.

Izzet Kale (M'88) received the B.Sc. degree (with honors) in Electrical and Electronic Engineering from the Polytechnic of Central London, London, U.K., the M.Sc. degree in The Design and Manufacture of Microelectronic Systems from Edinburgh University, Edinburgh, U.K., and the Ph.D. degree in Techniques for Reducing Digital Filter Complexity from the University of Westminster, London, U.K.

Since 1984, he has been with the staff of the University of Westminster, where he is currently a Professor of applied DSP and VLSI Systems, the Founder and Director of the Applied DSP and VLSI Research Group, where he has undertaken numerous applied research and development projects and contracts for European, U.S., and Japanese corporations working on innovative silicon-integrated product development for commercial applications. His research and teaching activities include digital- and analog-signal processing, silicon circuit and system design, digital-filter design and implementation, and A/D and D/A sigmadelta converters. He is currently working on efficiently implementable ultralowpower DSP algorithms/architectures and sigmadelta modulator structures for use in the communications and biomedical industries as well as hybrid Global Navigation Satellite Systems GPS/Galileo receiver structures and systems.